Photo–double-ionization of the *ns* shell of rare gases

L. Argenti,[1] P. Bolognesi,[2] R. Colle,[1] V. Feyer,[2,*] and L. Avaldi[2,3]
[1]*Dipartimento di Chimica Applicata e Scienza dei Materiali, Università di Bologna, 40136 Bologna, Italy*
[2]*CNR-IMIP, Area della Ricerca di Roma 1, CP10, 00016 Monterotondo Scalo, Italy*
[3]*CNR-INFM-TASC, Gas Phase Beamline@Elettra, Area Science Park, Trieste, Italy*
(Received 30 March 2009; published 16 June 2009)

The triple differential cross sections (TDCS) for the photodouble ionization of He, Ne, Ar, and Xe leading to the $He^{2+}(1s^{01}S^e)$, $Ne^{2+}(2s^02p^{61}S^e)$, $Ar^{2+}(3s^03p^{61}S^e)$, and $Xe^{2+}(5s^05p^{61}S^e)$ states have been measured at about 20 eV above their respective thresholds with the two photoelectrons equally sharing the excess energy. The experimental data are analyzed using a parametrization recently proposed [J. Phys. B **41**, 245205 (2008)] which takes into account experimental uncertainties. The parametrization provides a satisfactory representation of the shape of the measured TDCS. The study of the behavior of the gerade amplitude of the TDCS in the different targets gives hints on the dependence of the electron correlation with the principal quantum number n of the ionized ns orbital.

DOI: 10.1103/PhysRevA.79.063408 PACS number(s): 32.80.Fb

I. INTRODUCTION

A single photon with sufficient energy may excite more than one electron when it is incident upon an atom. For example, two electrons may be promoted to unfilled orbitals (double excitation), or they may be ejected leading to double ionization (double escape). In order to be involved in such a process the electrons have to interact strongly with each other and indeed these processes are dominated by electron correlations. Consequently, studies of double excitation and double ionization by photon impact provide unique information on electron correlations and this has aroused much interest in them [1–3]. The study of electron correlation in photon impact experiments has some advantages with respect to similar studies in processes induced by charged particles. The angular momentum and the energy of the photon are well defined. The polarization of the incident radiation provides a natural quantization axis and introduces convenient symmetries for the processes. Furthermore, within the dipole approximation, the number of final states is limited by the optical selection rules. Against this background photodouble ionization (PDI) in He, for example, provides a particularly clean system to study the fundamental three-body Coulomb problem [1], which has far reaching interest in many areas of the physical sciences. This target has only two electrons and the PDI results in a bare nucleus, an alpha particle and two free electrons. Electron correlations play a central role in determining both the initial-state wave function, that has been found to be important to evaluate the absolute cross section of the process, as well as the final-state wave function where they determine the motion of the two photoelectrons in the Coulomb field of the doubly charged residual ion. This three-body nature of the process also means that alternative theoretical approaches [4–7] must be sought since, for example, the independent-particle model is no longer applicable. The other neutral targets with only two electrons are the H_2 and D_2 molecules. Here the removal of the two electrons results in a complete explosion of the target, with four charged particles present in the final state. Thus the dynamics of the electron pair will depend on the alignment between the molecular axis and the polarization of the incident light, too [8–11].

A combined experimental and theoretical effort in the last years has lead to a satisfactory understanding of PDI in He an H_2 [3,11]. In the case of other targets, like the rare gases heavier than He, the situation is not as satisfactory. Indeed, despite a few sets of experimental data have been presented in the literature [12,13], the presence of more that one final ionic state, the more complex initial state and the possibility of indirect double ionization have hampered the extension of *ab initio* or numerical theories to the calculations of the triple differential cross section $d^3\sigma/dE_1d\Omega_1d\Omega_2$ (TDCS) of photodouble ionization.

A representation of the TDCS can be achieved considering that, due to the invariance with respect to rotation around the electric vector direction of the incident radiation and the general properties of the spherical harmonics, the geometrical and dynamical factors of the TDCS can be separated. This leads to an exact parametrization of the TDCS [14], that for example in the case of the photodouble ionization of an initial s shell and an incident radiation that propagates along the $\mathbf{z}$ axis and is fully linearly polarized along the $\boldsymbol{\varepsilon}=\varepsilon\mathbf{x}$ axis can be written as

$$d^3\sigma/dE_1d\Omega_1d\Omega_2 \propto |a_g(E_1,E_2,\vartheta_{12})(\cos\vartheta_1+\cos\vartheta_2) + a_u(E_1,E_2,\vartheta_{12})(\cos\vartheta_1-\cos\vartheta_2)|^2, \quad (1)$$

where E_i and ϑ_i $(i=1,2)$ are the energies of the two photoelectrons and their angles of emission with respect to $\boldsymbol{\varepsilon}$, respectively, and ϑ_{12} is their relative angle. The complex amplitudes a_g and a_u are, respectively, symmetric and antisymmetric relative to the exchange of E_1 and E_2. The ϑ_{12} and energy dependence of these amplitudes includes all the physical information on the dynamics of the process, i.e., the

*Present address: Sincrotrone Trieste, Area Science Park, Trieste, Italy

effects of the electron-electron and electron-residual ion interactions.

The generalization of this result to an arbitrary state of the target atom has been obtained by Manakov *et al.* [15] and Malegat *et al.* [16]. Then Istomin *et al.* [17] have extended the parametrization in the case of He to include the lowest-order nondipole term of the transition operator. Recently Argenti and Colle [18] have proposed a parametrization which is based on a general expression of the transition amplitude between arbitrary states of the target atom and the parent ion, with the transition operator expressed at any order of its multipolar expansion. The major advantage of this expression, that in the dipole approximation is equivalent to those of [15,16], is that it is expressed only in terms of elementary angular functions (Clebsch-Gordan coefficients, spherical harmonics and $6j$ factors). This allows an easy implementation of the formula in a general algorithm for any kinematic condition and the development of a fitting procedure which takes into account also the finite instrumental resolution in the energy and angle measurements through the inclusion of few additional parameters. The latter results in a remarkable improvement of the representation of the data.

In this work a set of experimental data of the PDI of He, Ne, Ar, and Xe leading to the $He^{2+}(1s^{0\,1}S^e)$, $Ne^{2+}(2s^0 2p^{6\,1}S^e)$, $Ar^{2+}(3s^0 3p^{6\,1}S^e)$, and $Xe^{2+}(5s^0 5p^{6\,1}S^e)$ states measured at about 20 eV above their respective thresholds with the two photoelectrons equally sharing the excess energy is analyzed with this parametrization.

The paper is organized as follows. A brief description of the experimental setup and of the parametrization formulae are given in Secs. II and III, respectively. The experimental results and their representation via the parametrization of the TDCS proposed in [18] are presented and discussed in Sec. IV. Finally Sec. V is devoted to some conclusions.

II. EXPERIMENT

The experiments have been performed at the gas phase photoemission beam line [19] of the Elettra storage ring using the multicoincidence end station [20]. The incident radiation is provided by an undulator source and is 100% linearly polarized [19]. Two independently rotatable turntables are housed in the vacuum chamber. Seven hemispherical electrostatic spectrometers are mounted at 30° angular intervals on a turntable that rotates in the plane perpendicular to the direction, $\mathbf{z}$, of propagation of the incident radiation, while three other spectrometers are mounted at $\vartheta_1=0°$, 30°, and 60° with respect to the polarization vector $\boldsymbol{\varepsilon}$ of the light on a smaller turntable. In these measurements both arrays have been kept in the perpendicular plane, i.e., in the dipolar plane, and all the analyzers have been set for the detection of electrons of the same kinetic energy, $E_1=E_2\approx 10$ eV. The energy resolution in these measurements was $\Delta E_{1,2}=0.250$ eV while the angular acceptances in the dipolar and perpendicular planes were $\Delta\vartheta_{1,2}=\pm 4°$ and $\Delta\varphi_{1,2}=\pm 3°$, respectively. The main part of the coincidence electronics is made by three independent time-to-digital converters, TDC. In the experiment each TDC unit is operated in the common start mode with the signal of each one of the three analyzers of the small turntable used as starts and the signal from the other seven as stops. In this way 21 coincidence pairs are collected simultaneously. The angular distribution is obtained by successive rotations of the larger frame. The relative efficiency of the spectrometers has been calibrated via the measurement of the photoelectron angular distribution of $He^+(n=3)$ at 10 eV above its threshold. At this energy the β value is known [21]. Then the obtained efficiencies have been confirmed by determining the β of the photoelectron angular distribution of $He^+(1s^{-1})$ at the same electron kinetic energies. The same efficiency correction has been assumed for the coincidence measurements. The validity of this assumption has been tested by measuring the coincidence yield at two positions of the larger turntable which allow to overlap two nearby analyzers. Because this calibration procedure has been applied to the rotatable spectrometers as well as to the "fixed" ones, all the experimental data at the three different ϑ_1 angles, even though not absolute, are internormalized and can be reported on a common scale of counts.

The double-ionization potentials of the $Ne^{2+}(2s^{-0}2p^6)$, $Ar^{2+}(3s^{-0}3p^6)$, and $Xe^{2+}(5s^{-0}5p^6)$ states are at 121.9, 74.4 and 59.2 eV, respectively. These energies are smaller than the respective binding energies of the ^4S ground state of the triply charged ion [22]. Thus the decay to the triple continuum is not allowed. Moreover care has been taken to check that no resonances, which may lead to photodouble ionization via an indirect process, were located at the photon energy used in the different experiments. To this purpose in the case of the experiment on Xe $(5s)$ the kinetic energy of the two photoelectrons has been increased of about 1 eV in order to avoid a too high random coincidence background due to the excitation of the $4d\rightarrow\varepsilon f$ giant resonance.

III. PARAMETRIZATION METHOD

The triple differential cross section of the photodouble ionization process produced by an incident photon of frequency ω and polarization direction $\boldsymbol{\varepsilon}$ is given in dipole approximation by

$$\frac{d^3\sigma}{dE_1 d\Omega_1 d\Omega_2} = \frac{4\pi^2}{c\omega}\frac{k_1 k_2}{\Pi^2_{L_0 S_0}}\sum_{M_\alpha\Sigma_\alpha}\sum_{\sigma_1\sigma_2}\sum_{M_0\Sigma_0}|\langle\psi^-_{\alpha;\vec{k}_1\sigma_1\vec{k}_2\sigma_2}|\vec{\varepsilon}\cdot\vec{p}|\phi_0\rangle|^2, \tag{2}$$

where $\vec{p}=\Sigma_{i=1}^N\vec{p}_i$ and ϕ_0 and $\psi^-_{\alpha;\vec{k}_1\sigma_1\vec{k}_2\sigma_2}$ are, respectively, the initial and final states of the atom with two outgoing electrons of linear momenta $(\vec{k}_1,\vec{k}_2)$ and spin projections (σ_1,σ_2). The TDCS is averaged upon the possible orientations of the target atom and summed upon the degenerate final states α of the parent ion. The quantum numbers $L_{0/\alpha}$, $S_{0/\alpha}$, $M_{0/\alpha}$, and $\Sigma_{0/\alpha}$ are those of the angular momentum, spin and their projections for the target atom (0) and parent ion (α) respectively, and $\Pi^2_{L_0S_0}=(2L_0+1)(2S_0+1)$ is the target degeneracy. *Ab initio* calculations of final continuum states sufficiently accurate for a quantitative comparison with experiments are actually possible only for the two-electron targets. This is

mainly due to the difficulty to take into account properly the electron correlations which play a crucial role in the PDI processes. An alternative way to the *ab initio* calculations is to reproduce the measured angular distributions through a parametrized expression of the TDCS in which kinematical and dynamical factors have been disentangled exploiting the constraints imposed by the symmetry of the transition matrix element in Eq. (2). In this approach, the $a_{g,u}$ dynamical factors, which are expressed in terms of transition matrix elements obtainable from *ab initio* calculations, are used as fitting parameters to reproduce the experimental TDCS. Knowledge of the dynamical parameters is useful in many respects, but especially to identify the main contributions to the TDCS and their dependence on quantum numbers. Different analytic expressions of the transition matrix element in Eq. (2) have been proposed to disentangle dynamical and kinematical contributions [15–18], but for the simplest case in which the initial state of the atom and the final state of the parent ion are both ^1S states, all the proposed parametrizations of the TDCS reduce to the well-known Eq. (1). The complex gerade and ungerade amplitude of Eq. (1) can be expressed in terms of the derivatives $P'_\ell(\cos\,\vartheta_{12})$ of the Legendre polynomials and the reduced transition matrix elements

$$a_{g/u}(k_1,k_2,\vartheta_{12}) = \sum_\ell \frac{(-1)^\ell}{\sqrt{\ell+1}}[P'_{\ell+1}(\cos\,\vartheta_{12}) \mp P'_\ell(\cos\,\vartheta_{12})] \times \frac{1}{4}\sqrt{\frac{k_1 k_2}{c\omega}}[\langle \psi^-_{\ell+1k_1,\ell k_2}||p_1| \times|\phi_0\rangle \pm \langle \psi^-_{\ell+1k_2,\ell k_1}||p_2||\phi_0\rangle]. \quad (3)$$

In real calculations the sum in Eq. (3) is truncated to a chosen $\ell_{\max}$ which represents the highest angular momentum included in the calculation. Our fitting procedure [18] of the experimental TDCS utilizes Eqs. (1) and (3) with the reduced matrix elements $\{\langle \psi^-_{l+1k_i,lk_j}||p_i||\phi_0\rangle\}$ used as fitting parameters and it takes into account also the finite instrumental resolution of the experiment.

The angular acceptance of the detectors in the experiments cannot in principle be neglected, particularly nearby the node of the TDCS. Therefore the parametrized TDCS are convoluted with a Gaussian angular response function with full width at half maximum FWHM=8°.

$$\frac{d^3\sigma_C}{dE_1 d\Omega_1 d\Omega_2} = \int d\vartheta'_1 \int d\vartheta'_2 \frac{d^3\sigma}{dE_1 d\Omega_1 d\Omega_2}(\vartheta'_1,\vartheta'_2)P(\vartheta'_1;\vartheta_1,\sigma) \times P(\vartheta'_2;\vartheta_2,\sigma), \quad (4)$$

where

$$P(x';x,\gamma) = \frac{\exp[-(x'-x)^2/2\gamma^2]}{\sqrt{2\pi}\gamma}. \quad (5)$$

The convolution has been done only on the angular acceptance of the spectrometer in the dipolar plane. In the case of helium the convolution improves the quality of the fit to the experiment. For the heavier gases, instead, the improvement is generally modest.

In order to take into account the finite-energy resolution of the spectrometers a detuning of the kinetic energies of the two photoelectrons with respect to the "ideal" equal energy sharing $E=E_1=E_2$ has to be introduced. Due to energy conservation, a photoelectron of energy $E_1=E\pm\Delta E$ can contribute to the measured TDCS only if the other photoelectron has a matching opposite detuning, i.e., its energy is $E_2=E\mp\Delta E$. In such a case the fitting procedure has to account for this "unequal" energy sharing. In principle one should consider several (E_1,E_2) pairs within the energy resolution of the experiment and weight the corresponding results according to a Gaussian distribution. In fact such a procedure would be quite cumbersome and it is not expected to produce significant modifications of the results and thus it has not been applied. Thus the finite experimental energy resolution has been taken into account fitting the formula of the unequal energy sharing, with both the $a_{g,u}$ amplitudes as fitting parameters, to the experimental data.

IV. RESULTS AND DISCUSSION

A. Experimental results

All the experimental results are shown in Fig. 1. The error bar of each experimental point corresponds only to the statistical uncertainty. The data of the TDCS of He and Ne at 20 eV above threshold have been already reported and discussed [23,24]. The evolution of the TDCS with ϑ_1 results from the combined action of the symmetry properties of the emitted electron pair, which has the $^1P^\circ$ configuration for the removal of two electrons from an *s* orbital, and the Coulomb repulsion between the two photoelectrons. When the direction of one electron is fixed at an angle ϑ_1 with respect to the direction of polarization of the incident radiation the symmetry properties favor the forward emission of the other electron, $\vartheta_{12}<90°$, while the Coulomb repulsion will forbid it, favoring instead the backward emission, $\vartheta_{12}>90°$. These somewhat opposite requirements result in a He TDCS with two nodes at $\vartheta_{12}=0,180°$ and two lobes mainly located in the half plane $\vartheta_{12}>90°$, whose relative intensity depends on ϑ_1. As for the overall relative intensity of the TDCS it increases as ϑ_1 increases.

At variance with He, it is interesting to observe that in the heavier rare gases there is an increased intensity of the TDCS measured in the half plane $\vartheta_{12}<90°$, at $\vartheta_1=0°$. Additional lobes start to develop in Ne, growing in size in the Ar and then even more in Xe, where they appear to dominate the TDCS. The TDCS measured at $\vartheta_1=30°$ and 60° display a variation in both the width and shape of the lobes. The behavior of the relative intensity of the TDCS in the case of Ne and Ar is similar to He, being the TDCS measured at $\vartheta_1=60°$ of larger intensity with respect to the one at $\vartheta_1=0°$.

In the case of Xe the intensities of the three TDCS are almost the same and the node at $\vartheta_{12}=180°$ is partially filled. Considering that all the measurements have been done in the same experimental conditions the filling of the node cannot be ascribed to the energy and angular resolutions of the ex-

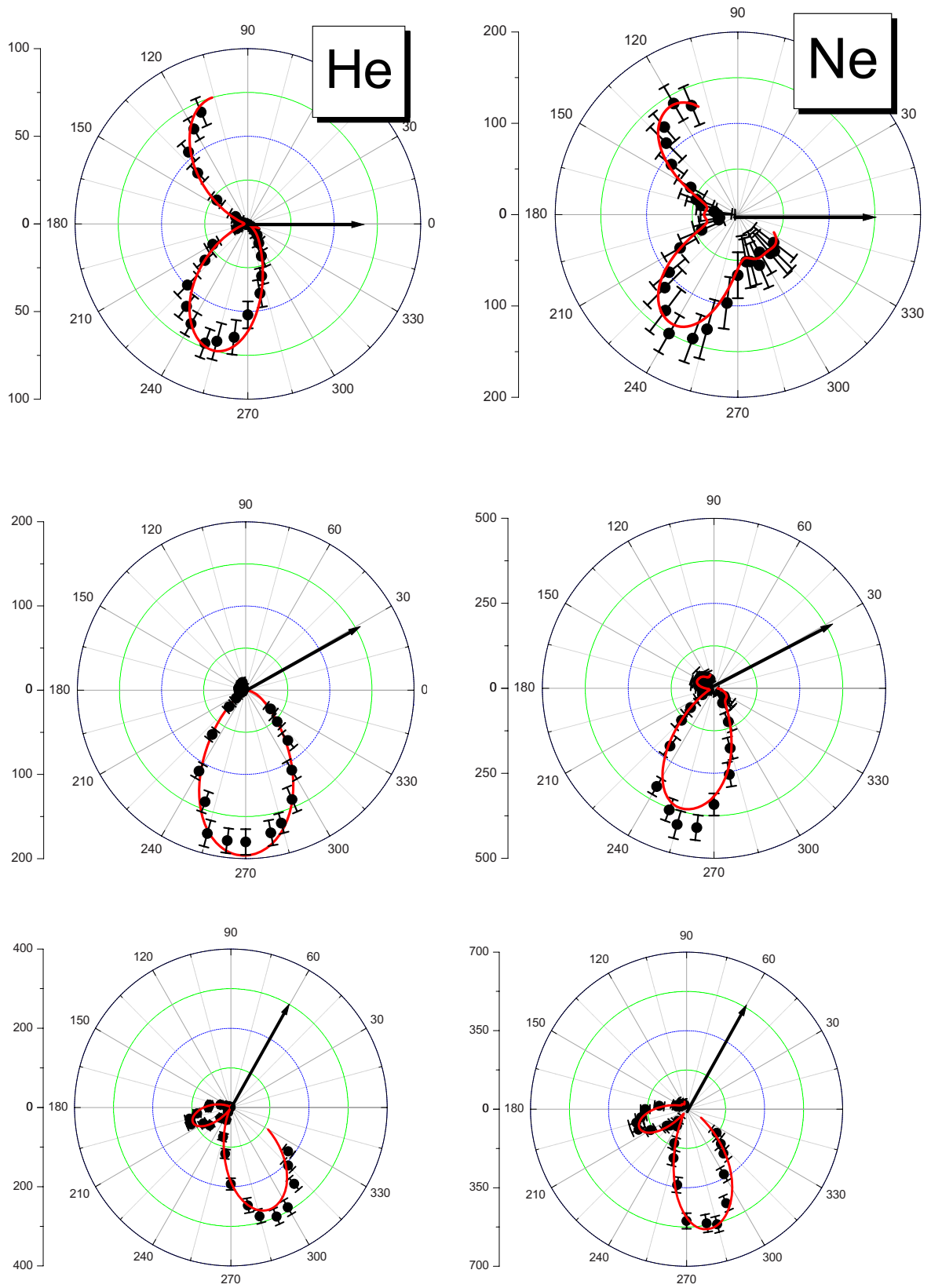

FIG. 1. (Color online) TDCS, for the photodouble ionization of He, Ne, Ar, and Xe leading to the $He^{2+}(1s^{0}{}^{1}S^{e})$, $Ne^{2+}(2s^{0}2p^{6}{}^{1}S^{e})$, $Ar^{2+}(3s^{0}3p^{6}{}^{1}S^{e})$, and $Xe^{2+}(5s^{0}5p^{6}{}^{1}S^{e})$ states measured at about 20 eV above their respective thresholds with the two photoelectrons equally sharing the excess energy and $\vartheta_1=0°$, 30°, and 60°, respectively. The line through the experimental points is the best fit to the data with the UES scheme (see text) and has been drawn here to guide the eyes.

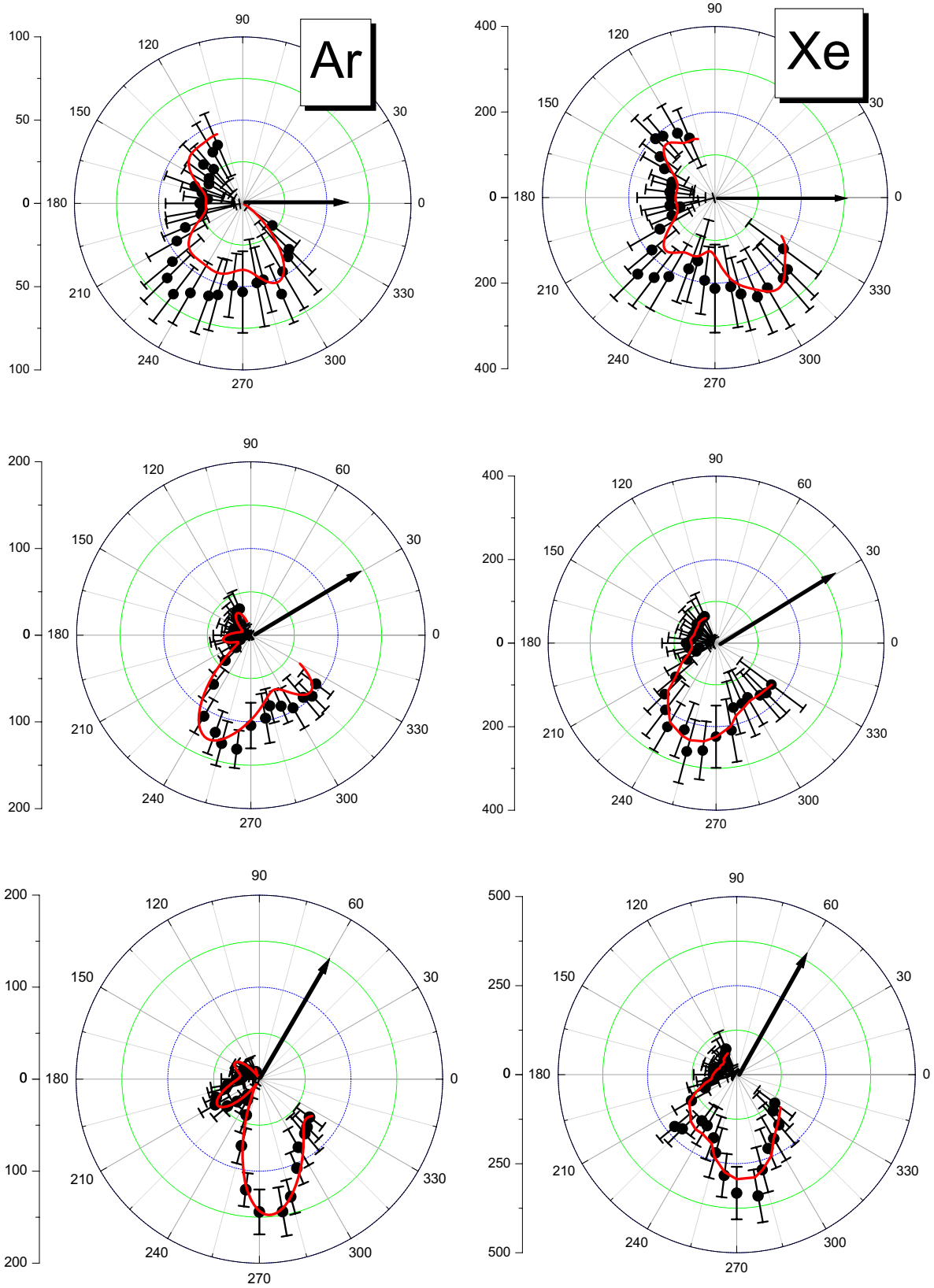

FIG. 1. (*Continued*).

periment. Vice versa both the observations can be considered an indication of the contribution of an indirect process. This may be a coupling of the direct double ionization with a decay mediated by the $4d \rightarrow \varepsilon f$ giant resonance. Indeed it is known by the measurements of the Xe total and partial cross sections that the giant resonance affects all the open channels [25].

B. Fitting method

The fit of the Eqs. (1)–(5) in Sec. III to the experimental data with the summations truncated to a selected $\ell_{\max}$ results in a nonlinear least-squares problem. The best values of the fitting parameters to be used in the representation of the TDCS are obtained by minimizing the reduced chi-square, χ^2, defined as

$$\chi^2 = \frac{1}{\Delta}\sum_{i=1}^{N_e}\left(\frac{y_i - d^3\sigma(\{x_1, \ldots, x_{N_p}\})/dE_1 d\Omega_1 d\Omega_2}{\sigma_i}\right)^2, \quad (6)$$

where σ_i is the uncertainty of the ith experimental point and Δ the number of degrees of freedom, given by the difference between the number (N_e=87) of experimental points $\{y_i\}$ and the number (N_p) of fitting parameters in the analytical expression of the TDCS. Being the experimental TDCS measured at the three different ϑ_1 values all internormalized, i.e., on the same relative scale of intensity, only one global fit for each target has been done. Thus N_e in Eq. (6) is the sum of experimental points of the three TDCS measured for each target. The numbers of fitting parameters when using the equal (EES) and unequal (UES) energy sharing formulas are $2\ell_{\max}-1$ and $4\ell_{\max}-1$, respectively. The absence of data in the region $\vartheta_{12}=0$ may lead to unphysical solution characterized by a lobe in the forward direction. To avoid this [18] a single fictious point at $\vartheta_1=0$ and $\vartheta_2=0$ has been added for each set of data. The uncertainty assigned to this point is of the same order of magnitude of the maximum of the experimental TDCS. At variance with Ref. [18] here no variation of ϑ_1 has been allowed. The presence of the normalization factor Δ in the definition of χ^2 is essential to compare consistently different fits of the same experimental data set performed with a different number of fitting parameters.

In the present analysis, we fitted both the EES and UES formulas, i.e., switching off and on the ungerade term in Eq. (1), to the experimental data. We found that within the (EES) fitting scheme only one minimum value for χ^2 is obtained. However, for sufficiently large angular momenta, the set of fitting parameters producing this minimum χ^2 value is not unique, but there is a finite number of distinct solutions providing a degenerate minimum value of the χ^2. These solutions result in gerade amplitudes with the same absolute value but different phase factors, as one can predict and also verify from the calculations [18]. On the other hand, the minima of the χ^2 found in the UES fitting scheme are generally nondegenerate, but they occur in a number larger than the degeneracy of the unique minimum of the EES scheme. For example in the case of the fit to the TDCS of argon with $\ell_{\max}$=5 the unique, absolute minimum of the χ^2 found in the EES scheme is fourfold degenerate, while in the UES scheme there are seven local minima with different χ^2, all nondegenerate. In this case we choose as absolute minimum the one with the lowest χ^2.

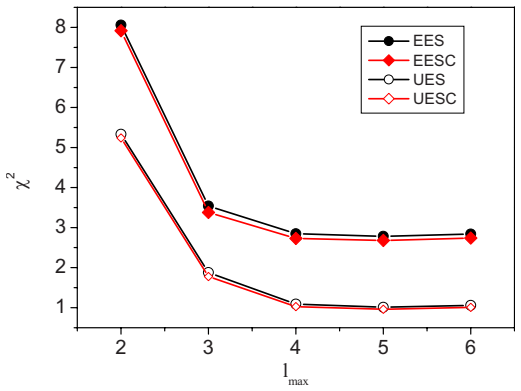

FIG. 2. (Color online) χ^2 values for the PDI of Ar to the $Ar^{2+}(3s^0 3p^6\,{}^1S^e)$ state as a function of $\ell_{\max}$ using the equal and unequal energy sharing schemes with (EESC and UESC) and without (EES and UES) the convolution with the experimental angular acceptance.

Here, we have used the TDCS of Ar (3s) as a test case for the different fitting schemes, varying the $\ell_{\max}$ value and taking into account the angular acceptance of the experimental setup. The variation in the χ^2 with $\ell_{\max}$ is shown in Fig. 2. The χ^2 displays a sharp decrease and then a plateau independently of the adopted fitting scheme. However, the results show that the representation in the EES scheme is unsatisfactory. The situation improves significantly using the UES scheme where a χ^2 of about 1 is reached at $\ell_{\max}$=5 (in the EES case χ^2 was larger than 3).

The convolution of the parametrized TDCS with the experimental angular uncertainty Eq. (5) slightly improves the quality of the fit. Indeed the χ^2 varies from 1.012 to 0.960 for $\ell_{\max}$=5, as can be seen in Fig. 2.

In order to explain better these findings we report in Fig. 3 the results of the different fitting schemes in the case of $\ell_{\max}$=5. The fit achieved with the EES scheme (panel a) is unable to represent some of the experimental features in the region ϑ_2=100–150° for the TDCS measured at ϑ_1=30 and 60°. The quality of the fit improves using the UES (panel b). The introduction of the experimental uncertainty via angular convolutions in the fitting scheme (panel c) does not lead to any appreciable differences, although the χ^2 decreases.

According to these findings, the UES scheme with the finite angular acceptance of the experiment taken into account has been adopted for all the targets. In all the studied cases, but Xe, the behavior of χ^2 versus $\ell_{\max}$ is the same and the plateau is achieved with $\ell_{\max}$=4 and 5 for He and Ne, respectively. In the case of Xe the value of χ^2 decreases continuously up to $\ell_{\max}$=7 where an acceptable value of 0.76 is reached and stabilized at $\ell_{\max}$=8. In this case, however, the quality of the fit is lower than for the other atoms as discussed in the next section. Despite the fact that the degrees of freedom in Xe with $\ell_{\max}$=8 is quite large (Δ=56), the extension of the expansion to larger ℓs is not meaningful, because the reduced χ^2 does not improve and the fitting function displays a large number of unphysical oscillations.

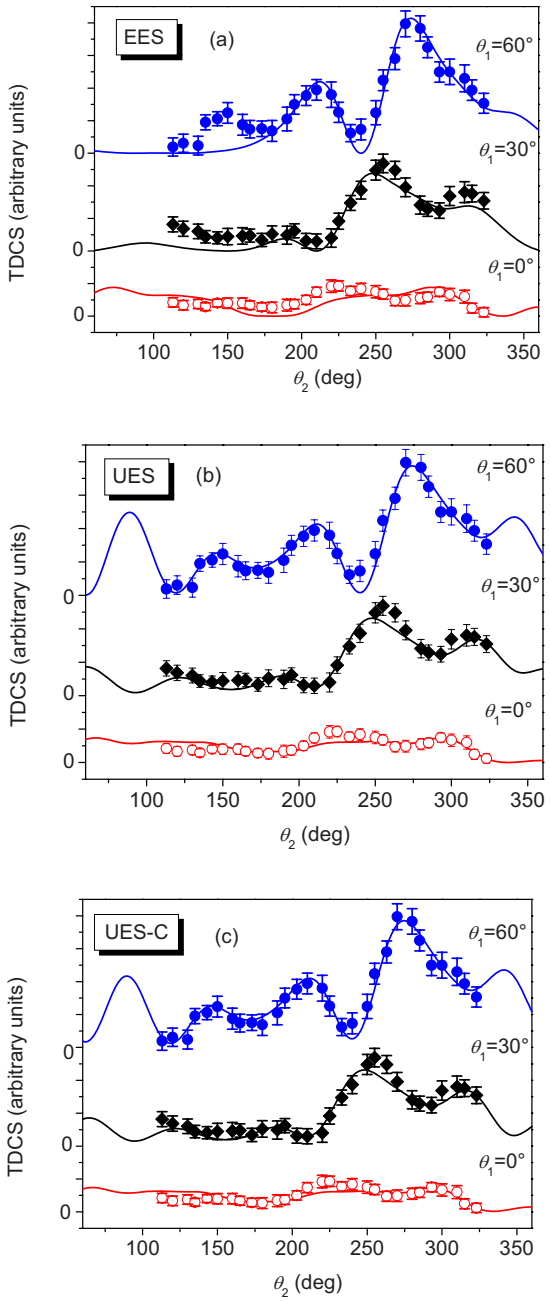

FIG. 3. (Color online) Comparison of the experimental TDCS of the $Ar^{2+}(3s^0 3p^6 {}^1S^e)$ state measured in equal-energy sharing at an excess energy of 20 eV with the results of the fit (full line) obtained using the equal-energy sharing scheme (panel a), the unequal energy sharing scheme (panel b) and the latter with the convolution with the angular acceptance of the spectrometer (panel c). In all the case the expansion has been limited to $\ell_{max}=5$.

C. Discussion of the results

The results of the best fit to the TDCS are reported in Figs. 4(a)–4(d) for He, Ne, Ar, and Xe, respectively. In each figure the three TDCS obtained at $\vartheta_1=0$, 30 and 60° are reported. The zero of the TDCS scale for each angular distribution has been shifted in order to show the quality of the fit without any overlap. The case of He is the only one where the convolution with the experimental angular acceptance improves significantly the χ^2, which varies from 1.7 to 1.1 after the convolution. This is due to the relevant role played by the node at $\vartheta_{12}=180°$ in the definition of the shape of the TDCS. The results displayed in Fig. 4 prove that the use of the present parametrization enables us to reproduce accurately all the features observed in the experiments. The evolution of the TDCS with ϑ_1 in the same target as well as the evolution of the shape in the studied series of targets is well reproduced. In the case of Xe at $\vartheta_1=0°$ and 60° despite the large uncertainty of the experiment the fit underestimates systematically the data in the region $200° \leq \vartheta_2 \leq 250°$.

The ℓ expansion of the gerade and ungerade amplitudes is understood as an expansion over the configuration ℓ (ℓ-1) of the electron pair. The value of ℓ_{max} depends on the initial-state configuration and the correlated dynamics of the PDI process. It provides a measure of the strength of the angular correlations [26]. While the problem of correlations in electron-impact excitation of highly excited Rydberg states has received considerable interest [27], only Malegat *et al.* [16] gave a determination of the ℓ_{max} in the case of the double continuum. However their interest focused on the change in ℓ_{max} as the excess energy above threshold increases and in the comparison with the predictions of Wannier models [28]. Here it is shown how the angular correlation involves more and more excited configurations of the electron pair as the atomic number of the target increases. Indeed the double ionization of an initial state with a single ns^2 configuration should lead to a unique $\varepsilon s \varepsilon p$ double continuum. The present results show that fg configurations can be involved in the case of He and configurations of the electron pair with even larger ℓ are needed to describe properly the angular distribution in the case of the other rare gases. In the case of He the higher ℓ configurations can result only from angular momentum exchange between the two photoelectrons in the continuum. In the other cases configurations different from ns^2 in the initial state may also contribute. This has been clearly shown in the case of the PDI of Ne 2*s* by Bolognesi *et al.* [24], where only the introduction of an initial state with a 2*p* contribution in the initial state, i.e., taking into account intershell correlation, allowed CCC theory [4] to represent satisfactorily the experimental TDCS.

In order to learn more about the dynamics of the PDI process and how this evolves in the series of studied targets, we have divided the raw experimental data by the $(\cos \vartheta_1 + \cos \vartheta_2)^2$ kinematical factor, which reflects the ${}^1P^\circ$ symmetry of the electron pair and the geometry of the experimental setup. Where multiple experimental determinations exist, a weighted average has been calculated. The results are shown in Fig. 5 where a logarithmic scale has been used to enhance the change in shape of the dynamical factor $|a_g(\vartheta_{12})|^2$ in the region of the smaller ϑ_{12}'s. The general behavior of the dynamical factor can be described in this way. In all cases it peaks at $\vartheta_{12}=180°$ and then decreases. However while in He the decrease is monotonic, in the case of Ne and Ar a second feature appears at about 70°–80°. In Xe a change in the slope is observed at about 120° and then the dynamical factor reaches a sort of plateau (within the experimental uncertainties) at $\vartheta_{12}<100°$.

In the literature, the dynamical factor for PDI in the equal-energy sharing experiments has been always repre-

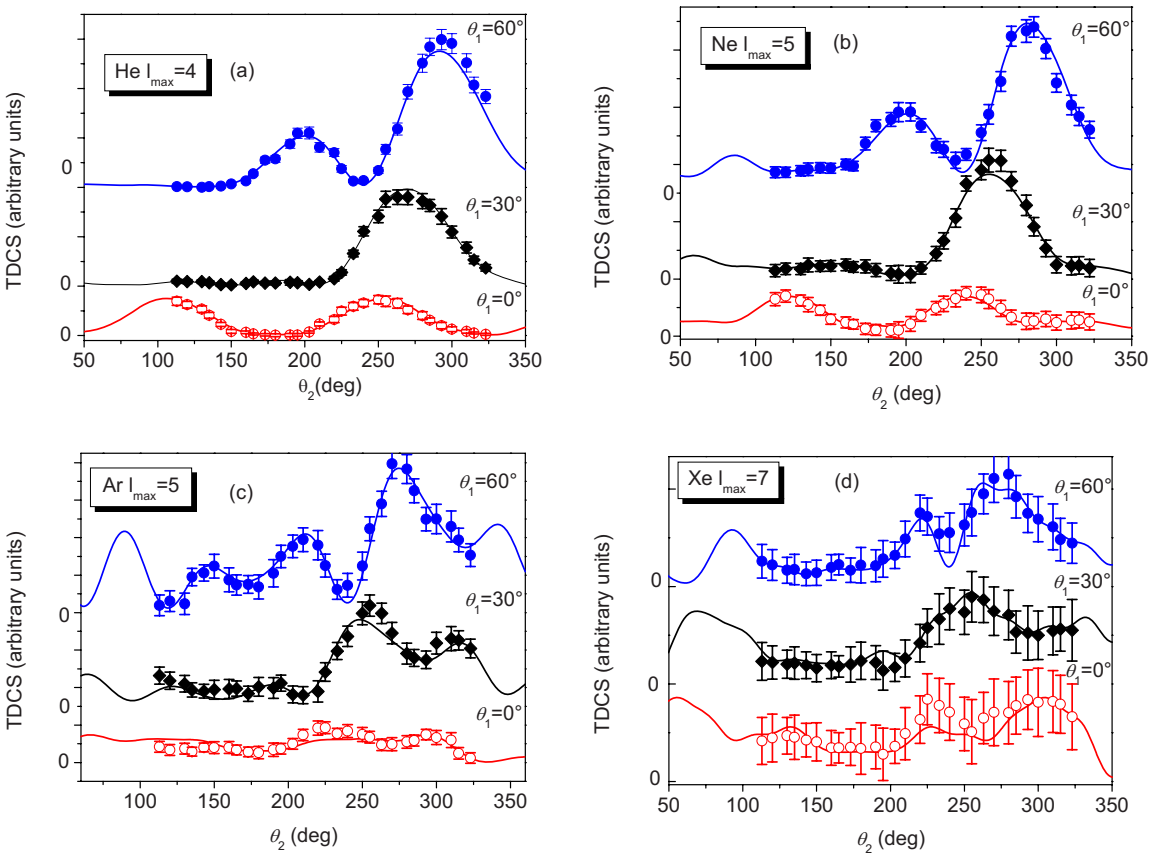

FIG. 4. (Color online) The experimental TDCS for the DPI of (a) He, (b) Ne, (c) Ar, and (d) Xe leading to the $He^{2+}(1s^{0}{}^{1}S^{e})$, $Ne^{2+}(2s^{0}2p^{6}{}^{1}S^{e})$, $Ar^{2+}(3s^{0}3p^{6}{}^{1}S^{e})$, and $Xe^{2+}(5s^{0}5p^{6}{}^{1}S^{e})$ states compared with results of the fit procedure (full lines) using the unequal energy sharing scheme and truncating the expansion to $\ell_{max}=4$, 5, 5, and 7, respectively.

sented by a Gaussian function. Indeed the Gaussian representation follows from the Wannier-type theories [28], where the angular variation near the Wannier saddle decouples from the radial motion. These models are expected to be valid only at small excess energies. However it turned out that the Gaussian approximation is a good description of several experimental results at higher excess energy [23], too. More recently Kheifets and Bray [29] supported the validity of the Gaussian parametrization via a fully numerical calculation in the range of excess energy 3–80 eV. At variance with this, a fitting procedure based on an exact parametrization, like this one or the ones presented by Manakov *et al.* [15] and Malegat *et al.* [16], gives access to the exact shape of the dynamical factor. The limit is imposed by the statistical accuracy of the experimental data and by the existence of a ϑ_{12} range inaccessible by the experiments. From the best values of the parameters obtained in the fit to the TDCS [see Eq. (3) and Fig. 4], the gerade $a_g(\vartheta_{12})$ functions have been calculated. Since the experimental data are on arbitrary scale, the $|a_g(\vartheta_{12})|^2$ values have been normalized to the experiments at $\vartheta_{12}=165°$. For sake of completeness also the $|a_u(\vartheta_{12})|^2$ obtained from the best values of the parameters of the fit are reported in the figure. The first observation is that the contribution of the ungerade amplitude is negligible all over the angular range where the experimental TDCS has a significant value. Moreover its shape is completely different from the one obtained in the analysis of a "generic" unequal energy sharing experiment according to the procedure introduced by Bolognesi *et al.* [30]. This confirms that the use of the unequal energy sharing scheme in the present analysis is not altering the physical description of the process. The rising of the $|a_u(\vartheta_{12})|^2$ at smaller ϑ_{12} may be an artifact of the procedure due to the lack of experimental points in that region. However the contribution of this part of the $|a_u(\vartheta_{12})|^2$ to the TDCS is negligible due to the rapid vanishing value of the ungerade kinematic factor as $\vartheta_{12}\rightarrow 0°$. The calculated $|a_g(\vartheta_{12})|^2$ well describe the shape of the experiments. In the case of He this confirms the previous findings [23,29,16] that a representation of the dynamical factor with a Gaussian function is a reasonable procedure while clearly shows the departure of the Gaussian approximation in the case of the rare gases heavier than He. This can be attributed to the different initial conditions. Indeed this was qualitatively predicted by Gailitis and Peterkop [31], then calculated by Malegat *et al.* [16] for the case of the PDI leading to the $Ne^{2+}(2p^{4})^{1}S^{e}$ state and finally observed in the case of $Ne^{2+}(2s^{0})^{1}S^{e}$ by Bolognesi *et al.* [24].

The main advantage of using a Gaussian function to represent the gerade amplitude is that its width can be used to characterize the correlated motion of the two electrons at a particular excess energy depending on the initial conditions. Thus we have represented the exact $|a_g(\vartheta_{12})|^2$ with a Gaussian function whose width has been fitted in the region where the correlation factor is not affected by the flattening ob-

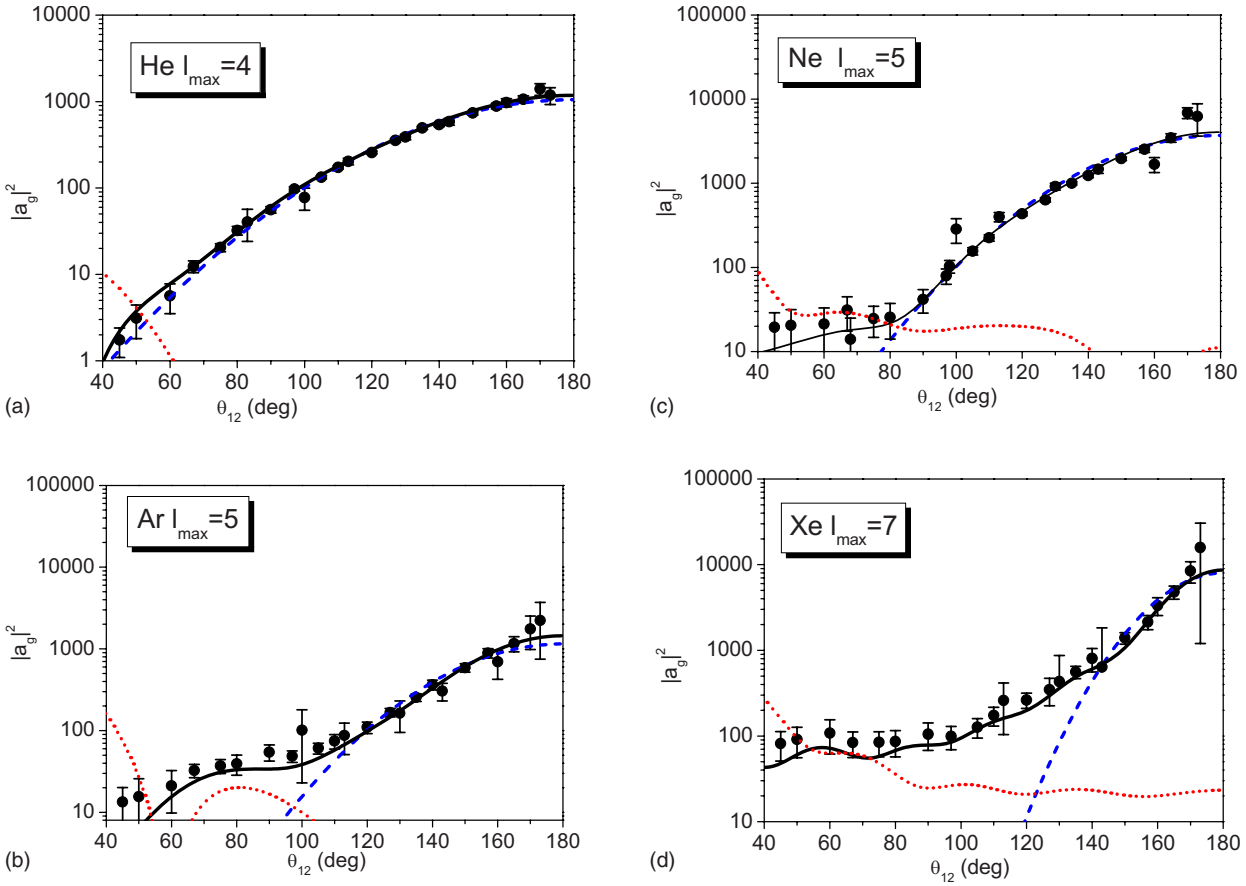

FIG. 5. (Color online) The experimental dynamical factor compared with the gerade (full line) and ungerade (dotted line) amplitudes reconstructed from the best values of the fit parameters for (a) He, (b) Ne, (c) Ar, and (d) Xe old. The fit with a Gaussian function (dashed line) is also reported (see text).

served in Fig. 5 and by the large uncertainties in the experimental data ($160° < \vartheta_{12} < 180°$). The FWHM obtained from this procedure are: $87 \pm 1°$ for He($1s$), $70 \pm 1°$ for Ne($2s$), $64 \pm 2°$ for Ar($3s$) and $39 \pm 5°$ for Xe($5s$). The values obtained for He and Ne are consistent with previous analysis of the present [23,24] and literature [23] data. The trend of the FWHM and the increase in $\ell_{\max}$ with the principal quantum number proves the increasing importance of the angular correlation in going from He($1s$) to Xe($5s$).

V. CONCLUSIONS

A set of data relative to the ejection of the two electrons from the *ns* shells of He ($n=1$), Ne ($n=2$), Ar ($n=3$), and Xe ($n=5$) at the same excess energy above their relative threshold have been measured and compared with a recently proposed parametrization procedure of the TDCS. The studied processes share the energy of the two photoelectrons and the symmetry of the initial and final states. Therefore they allow to follow the effect of the electron correlation on the shape of the TDCS as a function of the principal quantum number. The parametrization procedure and algorithm introduced by Argenti and Colle [18] proved to be very effective in order to extract from the full body of the experimental data the information on the angular momenta needed to describe the process, the "exact" complex amplitudes and the role of the electron correlation. This shows the usefulness of such a parametrization in all the cases where the present theories cannot predict the TDCS and suggests that the amplitudes built from the best fit parameters can be used in a direct comparison with the ones predicted by *ab initio* calculation. The limit of the analysis with parametric equations is that they do not allow to disentangle the contribution of the different initial conditions (description of the initial state) from the one due to the correlated dynamics of the two photoelectrons in the continuum. This can be solved only by proper *ab initio* calculations.

ACKNOWLEDGMENTS

Work partially supported by MURST-PRIN 2006 and FIRB "Probing the microscopic dynamics of chemical reactivity."

[1] J. S. Briggs and V. Schmidt, J. Phys. B **33**, R1 (2000).
[2] G. C. King and L. Avaldi, J. Phys. B **33**, R215 (2000).
[3] L. Avaldi and A. Huetz, J. Phys. B **38**, S861 (2005).
[4] A. S. Kheifets and I. Bray, Phys. Rev. A **54**, R995 (1996).
[5] L. Malegat, P. Selles, and A. K. Kazansky, Phys. Rev. Lett. **85**, 4450 (2000).
[6] D. A. Horner, J. Colgan, F. Martin, C. W. McCurdy, M. S. Pindzola, and T. N. Rescigno, Phys. Rev. A **70**, 064701 (2004).
[7] J. Colgan, M. S. Pindzola, and F. Robicheaux, J. Phys. B **34**, L457 (2001).
[8] T. Weber, A. O. Czasch, O. Jagutzki, A. K. Müller, V. Mergel, A. Kheifets, E. Rotenberg, G. Meigs, M. H. Prior, S. Daveau, A. Landers, C. L. Cocke, T. Osipov, R. Diez Muino, H. Schmidt-Böcking, and R. Dörner, Nature **431**, 437 (2004); **443**, 1014 (2006).
[9] W. Vanroose, F. Martin, T. N. Rescigno, and C. W. McCurdy, Nature **310**, 1787 (2005).
[10] M. Gisselbrecht, M. Lavollee, A. Huetz, P. Bolognesi, L. Avaldi, D. P. Seccombe, and T. J. Reddish, Phys. Rev. Lett. **96**, 153002 (2006).
[11] T. J. Reddish, J. Colgan, P. Bolognesi, L. Avaldi, M. Gisselbrecht, M. Lavollee, M. S. Pindzola, and A. Huetz, Phys. Rev. Lett. **100**, 193001 (2008).
[12] P. Bolognesi, G. C. King, and L. Avaldi, Radiat. Phys. Chem. **70**, 207 (2004) and references therein.
[13] P. Bolognesi, M. Coreno, G. Alberti, R. Richter, R. Sankari, and L. Avaldi, J. Electron Spectrosc. Relat. Phenom. **141**, 105 (2004).
[14] A. Huetz, P. Selles, D. Waymel, and J. Mazeau, J. Phys. B **24**, 1917 (1991).
[15] N. L. Manakov, S. I. Marmo, and A. V. Meremianin, J. Phys. B **29**, 2711 (1996).
[16] L. Malegat, P. Selles, and A. Huetz, J. Phys. B **30**, 251 (1997); L. Malegat, P. Selles, P. Lablanquie, J. Mazeau, and A. Huetz, *ibid.* **30**, 263 (1997).
[17] A. Y. Istomin, N. L. Manakov, A. V. Meremianin, and A. F. Starace, Phys. Rev. Lett. **92**, 063002 (2004).
[18] L. Argenti and R. Colle, J. Phys. B **41**, 245205 (2008).
[19] B. Diviacco, R. Bracco, C. Poloni, R. P. Walker, and D. Zangrando, Rev. Sci. Instrum. **63**, 388 (1992); P. Melpignano, S. Di Fonzo, A. Bianco, and W. Jark, *ibid.* **66**, 2125 (1995).
[20] R. R. Blyth, R. Delaunay, M. Zitnik, J. Krempasky, R. Krempaska, J. Slezak, K. C. Prince, R. Richter, M. Vondracek, R. Camilloni, L. Avaldi, M. Coreno, G. Stefani, C. Furlani, M. de Simone, S. Stranges, and M. Y. Adam, J. Electron Spectrosc. Relat. Phenom. **101-103**, 959 (1999).
[21] R. Wehlitz, B. Langer, N. Berrah, S. B. Whitfield, J. Viefhaus, and U. Becker, J. Phys. B **26**, L783 (1993).
[22] C. E. Moore, *Atomic Energy Levels*, NBS Ref. Data Series 35 (National Bureau of Standards, Washington, DC, 1971).
[23] G. Turri, L. Avaldi, P. Bolognesi, R. Camilloni, M. Coreno, J. Berakdar, A. S. Kheifets, and G. Stefani, Phys. Rev. A **65**, 034702 (2002).
[24] P. Bolognesi, R. Flammini, A. Kheifets, I. Bray, and L. Avaldi, Phys. Rev. A **70**, 062715 (2004).
[25] U. Becker, D. Szostak, H. G. Kerkhoff, M. Kupsch, B. Langer, R. Wehlitz, A. Yagishita, and T. Hayaishi, Phys. Rev. A **39**, 3902 (1989).
[26] U. Fano, Rep. Prog. Phys. **46**, 97 (1983).
[27] P. Hammond, F. H. Read, and G. C. King, J. Phys. B **17**, 2925 (1984).
[28] G. H. Wannier, Phys. Rev. **90**, 817 (1953).
[29] A. S. Kheifets and I. Bray, Phys. Rev. A **65**, 022708 (2002).
[30] P. Bolognesi, A. S. Kheifets, I. Bray, L. Malegat, P. Selles, A. Z. Kazansky, and L. Avaldi, J. Phys. B **36**, L241 (2003).
[31] M. Gailitis and R. Peterkop, J. Phys. B **22**, 1231 (1989).